

## SOLAR-BLIND DIAMOND DETECTORS FOR LYRA, THE SOLAR VUV RADIOMETER ON BOARD PROBA II

A. BENMOUSSA<sup>1,\*</sup>, J.-F. HOCHEDÉZ<sup>1</sup>, W.K. SCHMUTZ<sup>3</sup>, U. SCHÜHLE<sup>2</sup>,  
M. NESLÁDEK<sup>4,5</sup>, Y. STOCKMAN<sup>7</sup>, U. KROTH<sup>6</sup>, M. RICHTER<sup>6</sup>, A. THEISSEN<sup>1</sup>,  
Z. REMES<sup>4</sup>, K. HAENEN<sup>4,5</sup>, V. MORTET<sup>4</sup>, S. KOLLER<sup>3</sup>, J.P. HALAIN<sup>7</sup>  
R. PETERSEN<sup>5</sup>, M. DOMINIQUE<sup>1</sup> and M. D'OLIESLAEGER<sup>4,5</sup>

<sup>1</sup>Royal Observatory of Belgium, Circular Avenue 3, B-1180 Brussels, Belgium; <sup>2</sup>Max Planck Institut für Sonnensystemforschung – D-37191 Katlenburg-Lindau, Germany;

<sup>3</sup>Physikalisch-Meteorologisches Observatorium Davos – World Radiation Center, CH-7260 Davos Dorf, Switzerland; <sup>4</sup>Institute for Materials Research (IMO), Limburgs Universitair Centrum, Wetenschapspark 1, B-3590 Diepenbeek, Belgium; <sup>5</sup>Division IMOMEC, IMEC vzw, Wetenschapspark 1, B-3590 Diepenbeek, Belgium; <sup>6</sup>Physikalisch-Technische Bundesanstalt (PTB), Abbestr. 2–12, 10587 Berlin, Germany; <sup>7</sup>Centre Spatial de Liège – Avenue Pré Aily B-4031

Angleur – Belgium

(\*author for correspondence, e-mail: ali.benmoussa@oma.be; Tel.: +32 2 373 0276; Fax: +32 2 373 0224; <http://lyra-swap.oma.be/lyra>)

(Received 7 October 2004; accepted 30 December 2004)

**Abstract.** Fabrication, packaging and experimental results on the calibration of metal-semiconductor-metal (MSM) photodetectors made on diamond are reported. LYRA (Lyman- $\alpha$  Radiometer onboard PROBA-2) will use diamond detectors for the first time in space for a solar physics instrument. A set of measurement campaigns was designed to obtain the XUV-to-VIS responsivity of the devices and other characterizations. The measurements of responsivity in EUV and VUV spectral ranges (40–240 nm) have been carried out by the Physikalisch-Technische Bundesanstalt (PTB) in Germany at the electron storage ring BESSY II. The longer wavelength range from 210 to 1127 nm was measured with monochromatic light by using a Xe-lamp at IMO-IMOMEC. The diamond detectors exhibit a photoresponse which lie in the 35–65 mA/W range at 200 nm (corresponding to an external quantum efficiency of 20–40%) and indicate a visible rejection ratio (200–500 nm) higher than four orders of magnitude.

**Keywords:** diamond, solar-blind photodetector, UV detectors

### 1. Introduction

LYRA (Lyman- $\alpha$  Radiometer – Hochedez et al., 2005) is the solar VUV radiometer that will embark in 2006 onboard PROBA-2 (PROject for On-Board Autonomy), a technologically oriented ESA micro-mission conceived for the purpose of demonstrating new technologies (prototype payloads). LYRA will monitor the solar irradiance in four selected UV passbands. The channels have been chosen for their relevance to Aeronomy, Space Weather and Solar Physics (Rozanov et al., 2002):

(1) Lyman-alpha (121.6 nm), (2) the 200–220 nm Herzberg continuum range (interference filters for the two former passbands), (3) Al filter channel (17–70 nm) including He II at 30.4 nm, (4) Zr filter channel (1–20 nm), where solar variability is highest. LYRA will benefit from diamond detectors: it will be the first space assessment of a pioneering UV detector program (Hochedez et al., 2001). Diamond, a wide bandgap material (band gap energy  $E_g = 5.45$  eV), makes the sensors “solar-blind,” which allows avoiding some of the usual filters, that block the unwanted visible, but attenuate seriously the desired UV radiation. Therefore, their removal increases the effective area and therefore the signal-to-noise, the cadence, or an optimal trade-off of these two.

## 2. Devices operation

Metal-semiconductor-metal (MSM) photoconductive detectors are based on a planar configuration of the ohmic electrodes. An external voltage (5 V) is applied to the metal contacts generating an electric field (perpendicular to the incoming light) across the device. The incident radiation (photon) is directly absorbed in the diamond material, creating electron-hole pairs. As a consequence, the conductivity in the material increases, giving larger photocurrent. The performance (e.g. signal) of the diamond MSM detector depends significantly on the surface properties of the absorbing layer (diamond), on the applied voltage and the distance between electrodes (geometry design). The MSM detector differs from the p-i-n photodiode in several important ways. A p-i-n photodiode is a p-n junction with a doping profile tailored so that an intrinsic layer, the “i region,” is sandwiched between a “p layer” and “n layer”. It has a depleted region with a built-in electric field (parallel to the incoming light) that serves to separate photogenerated electron-hole pairs. A p-i-n photodiode produces a current proportional (linear) to the photon flux (while MSM is slightly sublinear) and can be operated in a photovoltaic mode (unbiased). The fact that the p-i-n diode operates in unbiased mode (i.e. it does not require an external voltage) implies a zero dark current.

## 3. Detector fabrication

A new circular MSM detector design using a Ti/Pt/Au multilayer structure for the interdigitated electrodes was investigated. The samples were designated MSM9-10-11 and 12 in the program and also in the sequel. Fabrication was carried out at IMO-IMOMECE facilities. A 0.8  $\mu\text{m}$  thick diamond layer was grown epitaxially on single IIa (natural) diamond substrates (500  $\mu\text{m}$  thickness), using microwave-plasma enhanced chemical vapor deposition (MECVD) technology. Details of the growth procedure can be found in Remes et al. (2005). A MSM detector is shown in Figure 1 with its rectangular ceramic ( $\text{Al}_2\text{O}_3$ ) package. This packaging (not

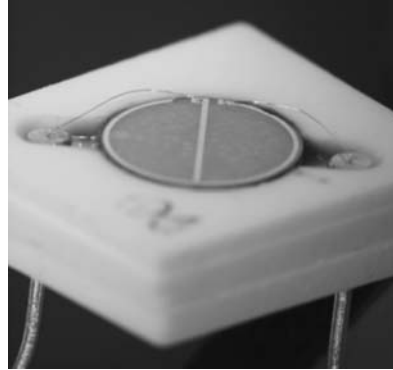


Figure 1. Photograph of the diamond MSM detector in its ceramic package.

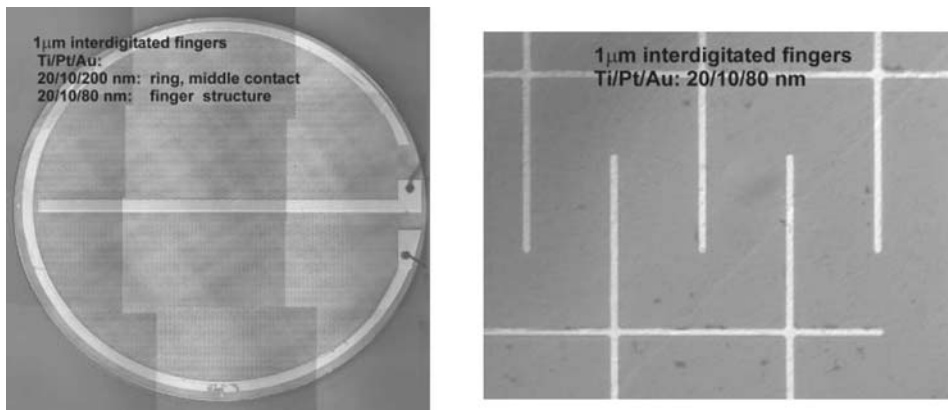


Figure 2. Optical image of Ti/Pt/Au contact structures on diamond.

commercially available) has the same dimensions as the Hamamatsu S1337-66BQ packaging.

A metal ring contact on the perimeter of the mesa defines the active area of the MSM photodetector, which has an inner diameter of 4.2 mm, corresponding to an optical detection area of 13.9 mm<sup>2</sup>. The optimisation of the circular contact geometry was done by “*Garching Analytics GmbH*” in Germany as shown in Figure 2. Metallization used to form contacts was Ti/Pt/Au with thickness 20/10/200 nm for the ring and middle contact and 20/10/80 nm for the fingers. The contact geometry has been chosen to ensure an optimised photo-carrier collection (highest fill factor) at 5 V. The metal fingers have been processed to be 1 µm in width with a spacing between the contacts as small as 5 µm. A new technique based on laser annealing was developed and optimized to improve the ohmic properties of titanium on diamond. It is a selective heating process at the interface metal (Ti)-diamond, which in turn allows to heat to significantly higher temperatures and therefore to better interdiffuse titanium and carbon.

#### 4. Measurements

The synchrotron radiation campaign was performed using the normal incidence monochromator (NIM) beamline of the Physikalisch-Technische Bundesanstalt (PTB) laboratory at the Berliner Elektronenspeicherung-Gesellschaft für Synchrotronstrahlung (BESSY II) over the spectral range from 40 to 240 nm. The detector calibration facility at BESSY II provides a synchrotron beam, monochromatized by a normal-incidence monochromator (with a spectral resolution of about 1% of the wavelength). To cover a wide spectral range from 40 to 240 nm, different filters and beamline mirrors are used to suppress higher order contributions to the selected bandwidth. This divides the entire range into three sub-ranges: 40–80 nm, 80–120 nm and 120–240 nm. Between these ranges, filters and mirrors are changed so that a spectral cleanliness is guaranteed to the level that higher order contributions are negligible. The detector calibration chamber at the end of the beamline is an ultrahigh vacuum chamber with manipulation stages, which allow the sample holder to be moved along three axes relative to the beam axis. The manipulation stages allow to raster the sample area and to toggle between test and reference detectors (a PtSi-Si Schottky photodiode, Richter et al., 2003). The spot size of the beam at the location of the samples is approximately  $1 \times 2$  mm, depending slightly on the chosen wavelength. The radiometric uncertainty of the measurements was estimated to be better than a few percent in absolute terms. Individual measurements were repeated to check stability and reproducibility. The data are corrected for the small decline (of 1%) of the current of the synchrotron storage ring during the time period of each measurement.

#### 5. Experimental results

##### 5.1. ABSOLUTE RESPONSIVITY (50–130NM)

One of the main parameters of semiconductor photodetectors is the responsivity, expressed in amps per watt (A/W). The responsivity is defined as the photocurrent per unit of incident optical power and described for the photoconductive detectors by the following expression:

$$R = \frac{I_{\text{ph}}}{P} = \frac{q\lambda}{hc} \eta G \quad (\text{A/W})$$

where  $I_{\text{ph}}$  is the detector photocurrent,  $P$  the incident power,  $q$  the electronic charge,  $\lambda$  the radiation wavelength,  $\eta$  the quantum efficiency (number of electron-hole pairs generated per incident photon) and  $G$  the photoconductive gain (number of carriers detected per photogenerated electron-hole pair) which can be significantly higher than 1. It is determined by the characteristics of the material (carrier lifetime,

mobility), the distance between the electrodes (inversely proportional) and the applied voltage. In this paper, the external quantum efficiency (EQE) is defined as  $\eta \times G$ .

The absolute spectral responsivity curves of samples designated as MSM9-10-11-12, under 5 V bias voltage, are shown in Figure 3. MSM detectors show a maximum at 200 nm of 45 mA/W for MSM9, 35 mA/W for MSM10, 53 mA/W for MSM11 and 66 mA/W for MSM12 corresponding to a 20–40% external quantum efficiency. It then slowly decreases towards 100 nm due to surface recombination. As seen in the figure, the responsivity increases slightly from 100 to 50 nm. The reproducibility looks good, i.e. 10 out of 13 detectors have spectral responsivities within the same magnitude.

The contribution of the photo-emission current (Saito, 2003) to the total signal of the MSM photodetector has been measured between 50 nm and 230 nm. In a typical set up for VUV measurements, the photodetector is housed in a metal vacuum chamber that is grounded to the earth and is usually common to the ground terminal of the electrometer. The photoelectrons emitted from the photodetector surface form an additional current circuit when electrons reach the vacuum chamber wall. To separate the contribution from the photoemission current, all measurements have been repeated with the other side grounded. In both cases, the same signal was measured. Thus, we conclude that there is no photo-emission contribution to the signal in this wavelength region.

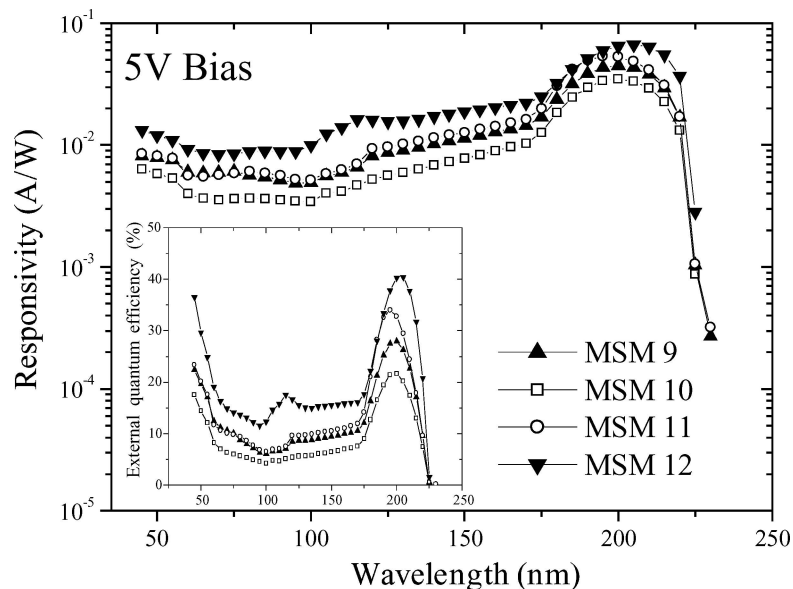


Figure 3. Absolute spectral response (in A/W) of MSM9-10-11-12 between 50 and 230 nm. The inset shows the external quantum efficiency EQE (%).

### 5.2. SOLAR-BLINDNESS TESTS (210–1127NM)

For the longer wavelength range from 210 nm, monochromatic light is generated by using a water cooled UV-enhanced 150 W Xe-lamp, a monochromator and filters. A schematic representation of the set up can be found in BenMoussa et al., 2004. For the low energy region the Xe-lamp is replaced by a halogen-lamp. The spectral responsivity of MSM9-10-11-12 measured in the explored wavelength range (50–1127 nm) is shown in Figure 4. The PTB-BESSY data (50–240 nm) agrees very well with the IMO-IMOMECE measurements (210–1127 nm). The MSM detectors show very similar sub-band gap responsivity with very high visible-to-UV suppression ratio of 4 orders of magnitude.

### 5.3. MSM VERSUS PIN

For the LYRA project, two types of diamond detectors are investigated: MSM (photoresistor) and pin (photodiode) detectors. The prototype pin2 diode has been described in a previous paper (BenMoussa et al., 2004). The responsivity of MSM9 at operational voltage of 5 V is compared with the pin2 photodiode (unbiased mode) in Figure 5. As we can see, MSM photodetectors offer an attractive benefit over alternative pin photodiodes especially between 120–220 nm (including Lyman- $\alpha$ ) where the responsivity is almost 1 order of magnitude higher compared to the pin2 photodiode. The pin2 exhibits a quantum efficiency ( $\eta$ ) of 7% at 200 nm. However,

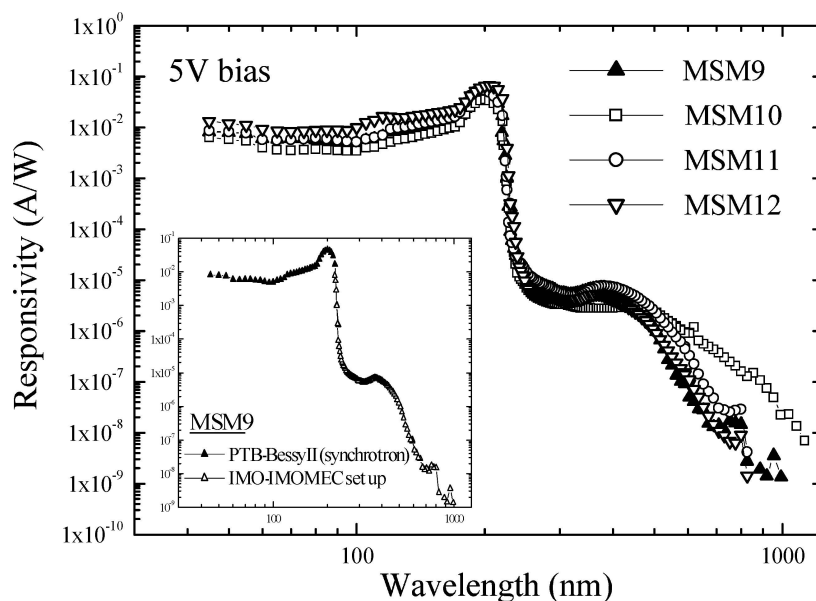


Figure 4. Measured spectral responsivity (in A/W) of MSM9-10-11-12 sample (50–1127 nm). The inset shows the responsivity of MSM9 with two different setups (PTB-Bessy II and IMO-IMOMECE).

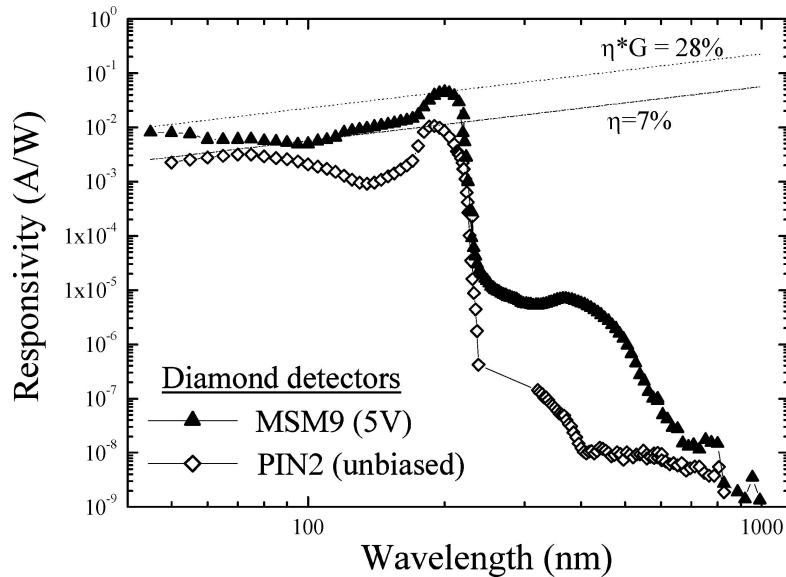


Figure 5. Absolute spectral responsivity (in A/W) of diamond MSM9 and pin2 samples.

MSM photodetectors display a UV/visible ratio (200/500 nm) over only four orders of magnitude while pin2 exhibits almost 6 orders. Moreover, pin detectors are faster devices due to their low capacitance, and they typically have no dark currents (background detrapping  $10^{-14}$  A). The MSM detectors show negligibly small (few pA) dark current over the area of the entire detector but some devices (3 out of 13) show an obvious persistent photoconductivity effect which may be related to surface defects.

## 6. Conclusion

Diamond MSM detectors with a photosensitive surface area of  $13.9 \text{ mm}^2$  ( $\text{Ø}4.2 \text{ mm}$ ) have been fabricated. The responsivity has been characterised thoroughly in the wavelength range of 1127–50 nm (1.1–24.8 eV). The characteristics of MSM detectors show the sharp diamond band edge around 220 nm and indicate a visible rejection ratio (200–500 nm) over more than four orders of magnitude. MSM diamond is a very sensitive material to VUV photons and suitable for space applications. Quantitative measurements (e.g. stability, linearity) have still to be carried out before the final definition of the channels and the selection of the flight model detectors.

## Acknowledgments

The authors wish to thank the Belgium Science Policy (BELSPO) for their financial support. The measurements at PTB/BESSY were made possible by a collaboration

between the Max-Planck-Institut für Sonnensystemforschung and the Physikalisch-Technische Bundesanstalt. We gratefully acknowledge the help of A. Gottwald of PTB. K. Haenen is a Postdoctoral Fellow of the Fund for Scientific Research – Flanders (Belgium, F.W.O.-Vlaanderen).

### References

- BenMoussa, A. et al.: 2004, *Phys. Status Solidi (a)* **201**(N11), 2536–2541.  
Hochedez, J.-F. et al.: 2001, *Diamond Relat. Mater.* **10**(3–7), 673–680.  
Hochedez, J.-F. et al.: 2005, *Adv. Space Res.*  
Remes, Z. et al.: 2005, *Diamond Relat. Mater.*  
Richter, M. et al.: 2003, *Metrologia* **40**, 107–110.  
Rozanov, E. et al.: 2002, 'Estimation of the ozone and temperature sensitivity to the variation of spectral solar flux.' In: A. Wilson (ed.), SOHO 11 Symposium: From Solar Min to Max: Half a Solar Cycle with SOHO, ESA SP-508, ESA Publications Division, Noordwijk, The Netherlands, p. 181.  
Saito, T.: 2003, *Metrologia* **40**, 159–162.